Supplemental Methods

Detailed case report

In April 2002, a 66 year old female, light former smoker (< 5 pack year smoking history) of mixed European descent was diagnosed with stage IV non-small cell lung cancer, adenocarcinoma with lepidic growth pattern. Her past medical history included neuroectodermal carcinoma of the lateral tongue treated with surgical resection, fibroid tumors of the uterus, hypothyroidism, chronic bronchitis, and mitral valve prolapse. Her family history was significant for a brother who was deceased from lung cancer. At the time of presentation she had dyspnea and heart palpitations. A CT scan demonstrated extensive dense parenchymal consolidation with air bronchograms involving a significant portion of the right lower lobe, and to a lesser extent the right middle lobe and lingula. She had a transbronchial biopsy and histopathology revealed well-differentiated adenocarcinoma, bronchioloalveolar type. She was treated from June to August 2002 with four cycles of gemcitabine and vinorelbine and had no response to therapy. In November 2003, she was started on gefitinib 250 mg daily and remained on therapy until December 2003 when she was admitted to hospital with a diagnosis of pneumonia and pneumonitis possibly related to gefitinib therapy. Her treatment was discontinued and she was discharged home with oxygen and hospice. She was relatively stable so in spite of being on hospice she sought a second opinion and in October 2005 she was started on bortezomib. After two cycles, she was still oxygen dependent and her CT scans demonstrated stable disease. In December 2005, she had increasing oxygen requirements and in January 2006 she underwent a right lower lobectomy for hypoxemia related to an intrapulmonary shunt in a completely involved right lower lobe. After surgery, her oxygenation improved significantly and was no longer requiring oxygen. In June 2006 she was enrolled on ECOG2501 and started on sorafenib 400 mg bid. After two months of therapy, her CT scans demonstrated a near complete response to therapy. Clinically she had improved dramatically, exercising daily. After three months of therapy, her sorafenib was reduced to 200 mg bid due to confusion attributed to therapy. She had also noted some skin discoloration. A biopsy in January 2010 of a residual apical lesion noted abundant acute inflammatory cells, and was negative for malignancy. In January 2011 she was admitted to hospital with pneumonia and upon discharge was once again oxygen dependent. She had a slow clinical progression and in July 2011 a CT scan demonstrated enlargement of a right lower lobe mass meeting RECIST criteria for progression. After 5 years on therapy, sorafenib was discontinued and she was started on carboplatin, paclitaxel and bevacizumab. She improved clinically after two cycles of chemotherapy but remained on oxygen and noted increasing fatigue. Her paclitaxel dose was reduced but she had worsening fatigue after her third cycle of chemotherapy and elected to have no further treatment. She was admitted to hospice and died in November 2011. At the time of relapse, she was the last remaining ECOG 2501 participant still receiving drug. She was one of only nine study responders, among 306 evaluable patients, and had by far the longest progression-free survival with other patients undergoing sorafenib treatment for two years or less.

Sequencing and Bioinformatics

We performed whole genome sequencing (WGS) of this patient's tumor and peripheral blood samples and whole transcriptome RNA sequencing (RNA-seq) of the tumor sample from this patient using Illumina massively parallel sequencing technology.   Tumor and normal genomic DNA were sequenced to 37.9X and 37.7X depth, respectively, and tumor RNA was sequenced to ~61X depth.   We compared tumor and normal WGS alignments to human genome build hg19 to identify somatic substitutions, insertions, and deletions(1). We used discordant paired-end and split-read mapping of WGS and RNA-seq data to identify rearrangement breakpoints(1). We additionally analyzed tumor and normal WGS read depth to obtain segmented copy number profiles and RNA-seq read depth to obtain gene expression estimates(1). Additional details of sample processing, sequencing, and bioinformatics are given below.

We obtained DNA from tumor and peripheral blood and tumor RNA from a fresh primary tumor resection specimen.   Informed consent and an ethical vote (Institutional Review Board) were obtained for this patient sample using protocols approved by the Broad Institute of Harvard and MIT and Vanderbilt University. We used standard Broad Institute protocols for DNA extraction and whole genome library construction. Libraries were sequenced on the Illumina HiSeq instrument to generate 101bp reads.   Alignments were processed and aligned to Human Genome Reference Consortium build 37 (GRCh37) using the Broad Institute "Picard" pipeline (http://picard.sourceforge.net).   BAM files produced by the Picard pipeline are available in dbGaP

under accession number phs000488.v1.p1.   We performed somatic variant calling using a custom middleware platform called "Firehose" (http://www.broadinstitute.org/cancer/cga/Firehose) containing algorithms for quality control, local realignment, substitution calling, small insertion and deletion identification, rearrangement detection, variant annotation, computation of mutation rates, and calculation of sequencing metrics.   This included specialized pipelines for somatic mutation detection, rearrangement calling, and copy number breakpoint detection(2-4).   Additional WGS germline variant analysis was performed using the Genome Analysis Toolkit (GATK(5), http://www.broadinstitute.org/gatk/), including UnifiedGenotyper for mutation and insertion-deletion detection and VariantQualityScoreRecalibration pipelines for statistical quality control filtering of variants.   Annotation of germline and somatic sequence variants was performed using Oncotator (http://www.broadinstitute.org/oncotator/).   Alignments for known lung adenocarcinoma oncogenes were reviewed for substitutions and small indels (*KRAS*, *EGFR*, *BRAF*, *ERBB2*, *PIK3CA*) and gene fusions (*ALK, ROS1,* and *RET*).

RNA sequencing was performed using the Illumina TruSeq mRNA Sample Preparation Kit to convert the mRNA in 100 ng of total RNA into a library of template molecules suitable for subsequent cluster generation and sequencing on an Illumina HiSeq 2000 with poly-A enrichment and cDNA was generated using SuperScript II reverse transcriptase and random primers. This is followed by second strand cDNA synthesis using DNA Polymerase Iand RNase H followed by ligation with Illumina multiplexing adapters. The flow cell was loaded onto the Illumina HiSeq 2000 utilizing v3 chemistry and HTA 1.8. The raw sequencing reads in BCL format are processed through CASAVA-1.8.2 for FASTQ conversion and demultiplexing.   The RTA chastity filter is used and only the PF (passfilter) reads are retained for further analysis. Short reads were aligned to the GRCh37 and hg19 knownGene UCSC transcript models using TopHat.   Gene expression analysis and somatic mutant quantification was performed using Cufflinks(6) (http://cufflinks.cbcb.umd.edu/index.htm), samtools(7) (samtools.sourceforge.net) and R Bioconductor packages (www.bioconductor.org).   Visualizations were generated using CIRCOS(8) (www.circos.ca) and R (http://www.r-project.org/).

Retroviral transduction

Wild-type *ARAF* or *RAF1* was mutagenized and cloned into pDONR223 by recombination of PCR products, then transferred to a Gateway-adapted (Invitrogen) pBabe puro expression vector(9). Amphotropic virus was produced by cotransfection of pBabe constructs with pCL-Ampho (Imgenex) in 293T cells. AALE cells were infected with amphotropic virus and selected with 1 μg/ml puromycin two days after transfection. Ecotropic virus used for infection of NIH-3T3 cells was produced similarly, but by cotransfection of 293T cells with pCL-Eco (Imgenex). 293T cells were maintained in DMEM (Corning Cellgro) supplemented with 10% fetal bovine serum (Gemini Bioproducts), and NIH-3T3 were maintained in DMEM supplemented with 10% bovine serum (Gibco). AALE cells were grown in SAGM (Lonza).

Soft agar assays

$5x10^4$ cells were suspended in media containing 0.33% Select Agar (Invitrogen) and plated on a bottom layer of media containing 0.5% Select Agar in a 6-well plate. EGF was removed from the SAGM defined media for the AALE soft agar assays to reduce background.   Plates were incubated at 37° C 2-3 weeks prior to imaging. Inhibitors were purchased commercially (Selleck Chemicals) and added directly into the top agar layer during plating. Colonies were photographed and quantified using the Cell Profiler open-source software(10). IC_{50}s and 95% confidence intervals were calculated using the Prism software (Graphpad).

Immunoblotting

Cells were lysed in a buffer containing 50 mM Tris- HCl (pH 7.4), 150 mM NaCl, 2.5 mM EDTA, 1% Triton X-100, and 0.25% IGEPAL CA630. Protease inhibitors (Roche) and phosphatase inhibitors (Calbiochem) were added prior to use.   Antibodies employed in immunoblotting are described in the supplementary methods. Immunoblotting was performed as described using the following antibodies: ARAF (Cell Signaling Technology 4432), BRAF (Cell Signaling Technology 5284), RAF1 (Cell Signaling Technology 9244), Mek (Cell Signaling

Technology 2352), phospho-Mek (Cell Signaling Technology 9154), Erk (Cell Signaling Technology 9107), phospho-Erk (Cell Signaling Technology 9101), and vinculin (Sigma V9264) (11).

GST-14-3-3ζ pulldown assays

AALE cells ectopically expressing wild-type or mutant ARAF were lysed in lysis buffer containing 20 mM Tris-HCl (pH 8.0), 137 mM NaCl, 2 mM EDTA, 1% IGEPAL CA630, and 10% glycerol. Protease inhibitors (Roche) and phosphatase inhibitors (Calbiochem) were added prior to use. 1 µg GST-14-3-3ζ (Sigma-Aldrich #SRP5155) was incubated with 500 µg each lysate for 2 hr at 4 °C. 10 µl glutathione agarose (Thermo Scientific #16100) was added and incubated with rotation for 1 hr at 4 °C. The glutathione agarose was pelleted by centrifugation and washed twice with lysis buffer. Pellets or 50 µg whole cell lysate were boiled in SDS sample buffer and supernatants loaded onto a 4-12% polyacrylamide gel. Immunoblotting was performed as described(11) with the following antibodies: ARAF (Cell Signaling Technology 4432) or pan-14-3-3 (Cell Signaling Technology 8312).

TCGA data

Mutation data from the cancer genome atlas (TCGA) was obtained from https://tcga-data.nci.nih.gov/tcga/. Tumor type abbreviations associated with this dataset are the following: luad = lung adenocarcinoma, skcm = cutaneous melanoma, coad = colorectal adenocarcinoma, stad = gastric adenocarcinoma, thca = thyroid carcinoma, ucec = uterine corpus endometrial carcinoma, lusc =lung squamous cell carcinoma, gbm = glioblastoma multiforme, brca = breast adenocarcinoma, hnsc = head and neck squamous cell carcinoma, kirp = kidney renal papillary cell carcinoma, blca = bladder carcinoma, read = rectal adenocarcinoma, lgg = lower grade glioma, prad = prostate adenocarcinoma, cesc = cervical squamous cell carcinoma, kirc:kirp = kidney renal clear cell carcinoma ov = ovarian carcinoma).

Statistics

IC50's were estimated from sorafenib and trametanib inhibition dose-response data using least squares non-linear regression. A transformation of the 4 parameter logistic model

$$y = B_{min} + \frac{B_{max} - B_{min}}{1 + \left(\frac{IC50}{x}\right)^{n}}$$

was fit by least squares to infer $IC50, B_{max}, B_{min}$, and n. Here, B_{max} and B_{min} represent maximal and minimal response, n is the Hill coefficient, x and y corresponds to dose and response (percentage maximal survival) data, respectively. 95% Confidence intervals (CI) on regression parameters were computed using approximate standard errors around the least-square estimates, and transformed into model parameters to yield $IC50$ CI's.

Supplemental Results
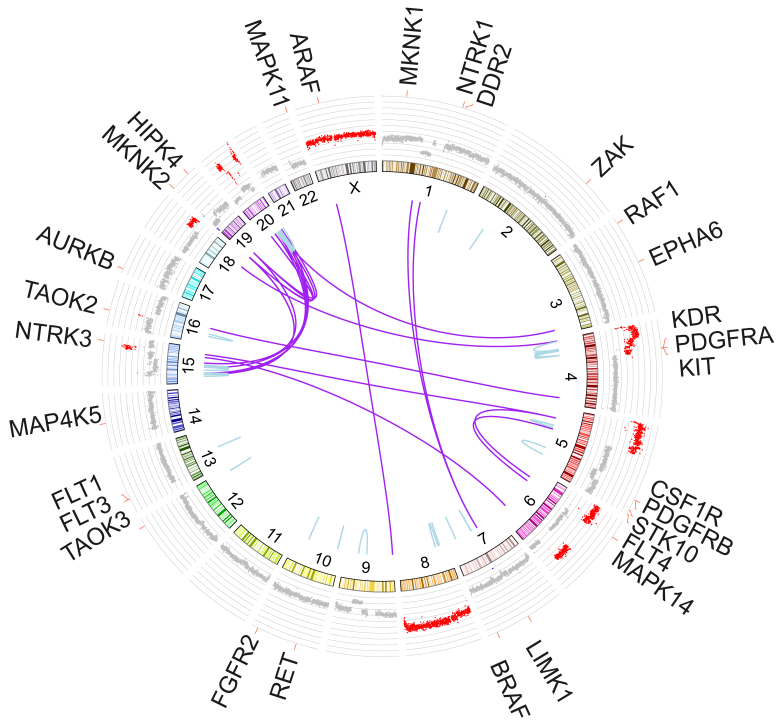
Mutation Spectrum Analysis

We employed massively parallel DNA sequencing of this patient's pre-sorafenib treatment resection tumor sample and normal adjacent tissue (Figure 1) to determine possible genetic alterations that may have been responsible for her sustained sorafenib response. Whole genome sequencing (WGS) of primary tumor (37.9X) and normal (37.7X) revealed 25,150 somatic mutations (8.7 mutations / MB). Among these, were 101 non-synonymous mutations affecting the coding regions of 99 genes, including 15 events predicted to have a truncating effect on mRNA translation. Copy number analysis revealed broad gains of multiple chromosome arms and an absence of focal amplification events (Supplemental Figure 1). 58 rearrangements were detected by WGS, including 2 frame-preserving gene fusion events. The somatic variant burden (with respect to mutation, rearrangement, and copy number alteration) was consistent with that of other lung adenocarcinomas profiled in large-scale lung adenocarcinomas profiled in large-scale genome surveys[12-21]. To verify this, we performed mutation-spectrum based clustering of the responder with other lung adenocarcinoma WGS cases from TCGA (TCGA (http://cancergenome.nih.gov/) and Imielinski *et al* lung adenocarcinoma datasets[21], and found that the responder WGS profile clustered closely among other ever-smokers (Supplemental Figure 2). Though all of the *ARAF* / *RAF1* mutant tumors in the TCGA lung adenocarcinoma data came from smokers, the C>G and C>T substitutions underlying these mutations do not represent the typical (C>A) smoking associated mutation signature[18, 21-23] (Supplemental Figure 2) . It is important to note that driver alterations can occur in atypical nucleotide context combinations (e.g. BRAF V600E, c.1799T>A in C>T predominant malignant melanoma)[24], a feature that is often used to provide a statistical signal of selection[22].

RAF1 Transformation Experiments

The functional effects of the *RAF1* mutations observed in lung adenocarcinoma were evaluated in both AALE and NIH-3T3 cells, due to the high background activity of wild-type *RAF1* and the difficulty in achieving equal levels of expression of all constructs in the AALE cells. *RAF1* p.S257L was strongly transforming in NIH-3T3 cells , but the p.S257W mutant exhibited only a slight gain of function over wild-type *RAF1* (Supplemental Figure 5, A,B). A *RAF1* p.S259A mutation, reported in ovarian cancer in the COSMIC database[25], was highly oncogenic, comparable to *RAF1* p.S257L and consistent with previous reports demonstrating that *RAF1* p.S259A is constitutively active[26]. A similar trend was observed in AALE cells, although the assay was not as robust in these cells due to poorly understood selective forces driving high expression of wild-type *RAF1* and the weakly oncogenic allele *RAF1* p.S257W (Supplemental Figure 5C, D). These results confirm that mutations of *RAF1* p.S257 are also activating, defining a novel oncogenic mutational hotspot in the *ARAF* and *RAF1* genes. The *RAF1* mutations were furthermore also sensitive to sorafenib and trametinib treatment, with IC50s comparable to those for the oncogenic *ARAF* mutants (Supplemental Figure 6A, B). As expected, phosphorylation of Mek and Erk was also downregulated upon treatment with sorafenib and trametinib, respectively (Supplemental Figure 6 C, D).
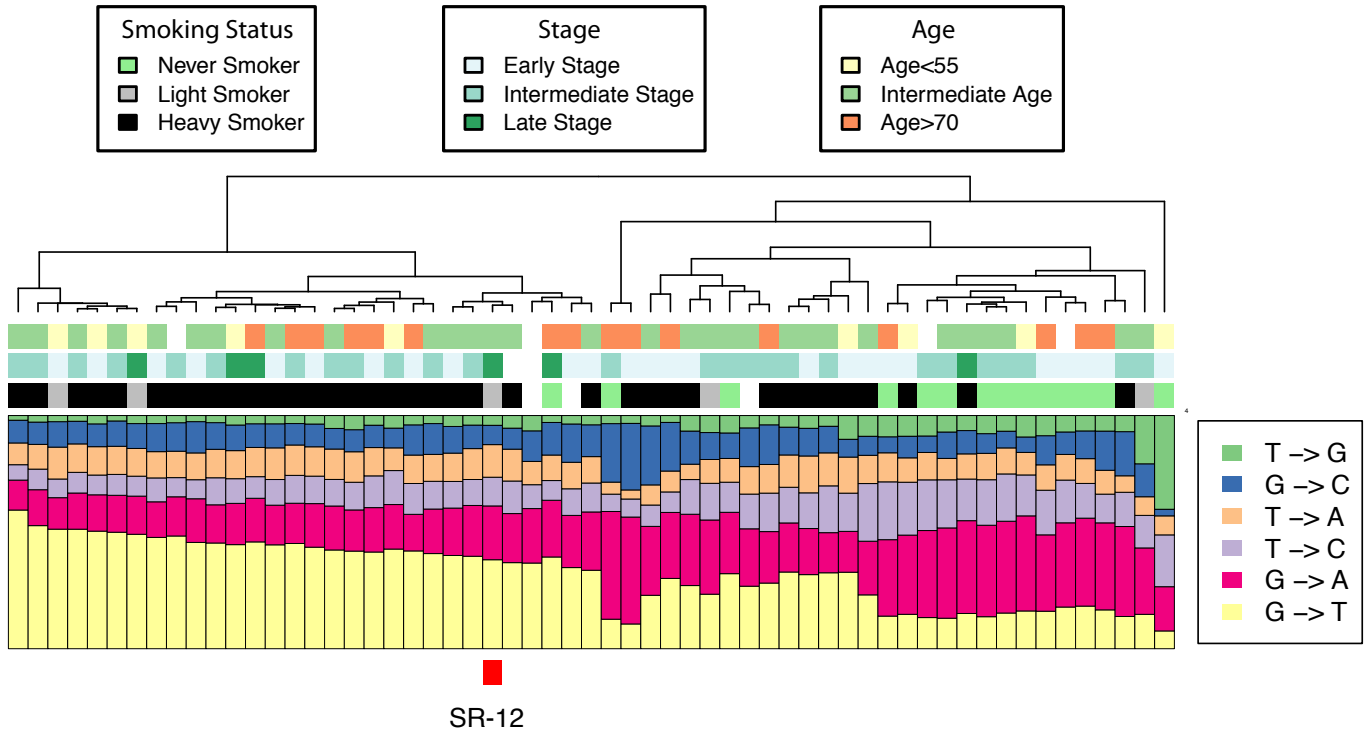
Supplemental Figures

<u>Supplemental Figure 1:</u> CIRCOS plot (www.circos.ca) (8) representing somatic inter- (purple) and intra- (blue) chromosomal rearrangements (inner links) and copy number changes (outer scatter track) detected by WGS, with locations of 29 known sorafenib targets labeled on the outer track.

Mutation spectrum clustering of sorafenib responder with 59 other lung adenocarcinoma cases profiled with whole genome sequencing in TCGA (http://cancergenome.nih.gov/) and Imielinski et al lung adenocarcinoma datasets(21). A mutation spectrum was computed for each case using the frequencies of somatic substitutions at each of six strand-collapsed nucleotide signatures (e.g. G→A), plotted as a stacked bar plot and color coded according to the legend on the right of the plot. Clinical features of patients are shown using three rows of color coded tracks above the stacked bar plot, with legends shown at the top of the plot. Patients (columns) were clustered based on the similarity of their spectra. Mutation spectra yield clusters that reflect both tumor type of origin and mutagen exposure(21, 22). In this analysis, the sorafenib responder clusters with other ever-smoker lung adenocarcinoma cases. The profile corresponding to the sorafenib responder (SR-12) is denoted by the red square below the plot.

SR-12

Supplemental Figure 3:

Matrix of mutations across known lung adenocarcinoma genes and 7 cases including SR-12 and cases from the TCGA (http://cancergenome.nih.gov/) and Imielinski et al lung adenocarcinoma datasets(21) showing CR2 hotspot mutations in *ARAF* and *RAF1* in our analysis. Gene labels are shown on the left and patient labels are shown below. Mutation types are color-coded according the legend at the right of the figure.

Inhibition of *ARAF* AALE soft agar colony formation correlates with a decrease in substrate phosphorylation. (A) MEK phosphorylation is decreased in response to sorafenib treatment. Immunoblots from AALE cells ectopically expressing *ARAF* mutants treated with the indicated concentrations of sorafenib for 4 hours. (B) Response of ARAF mutant AALE soft agar colony formation to the indicated concentrations of trametinib. (C) Dose response curves for data shown in (B). Data and error bars in panels (B),(C) represent mean ± SEM, respectively, obtained from triplicate experiments. (D) Erk phosphorylation is decreased in response to trametinib treatment. Immunoblots from AALE cells ectopically expressing *ARAF* mutants treated with the indicated concentrations of trametinib for 2 hours.

A

B

C

	ARAF wt	ARAF S214C	ARAF S214F	ARAF S214T
IC50 (nM)	1.2	1.9	2.1	2.1

D
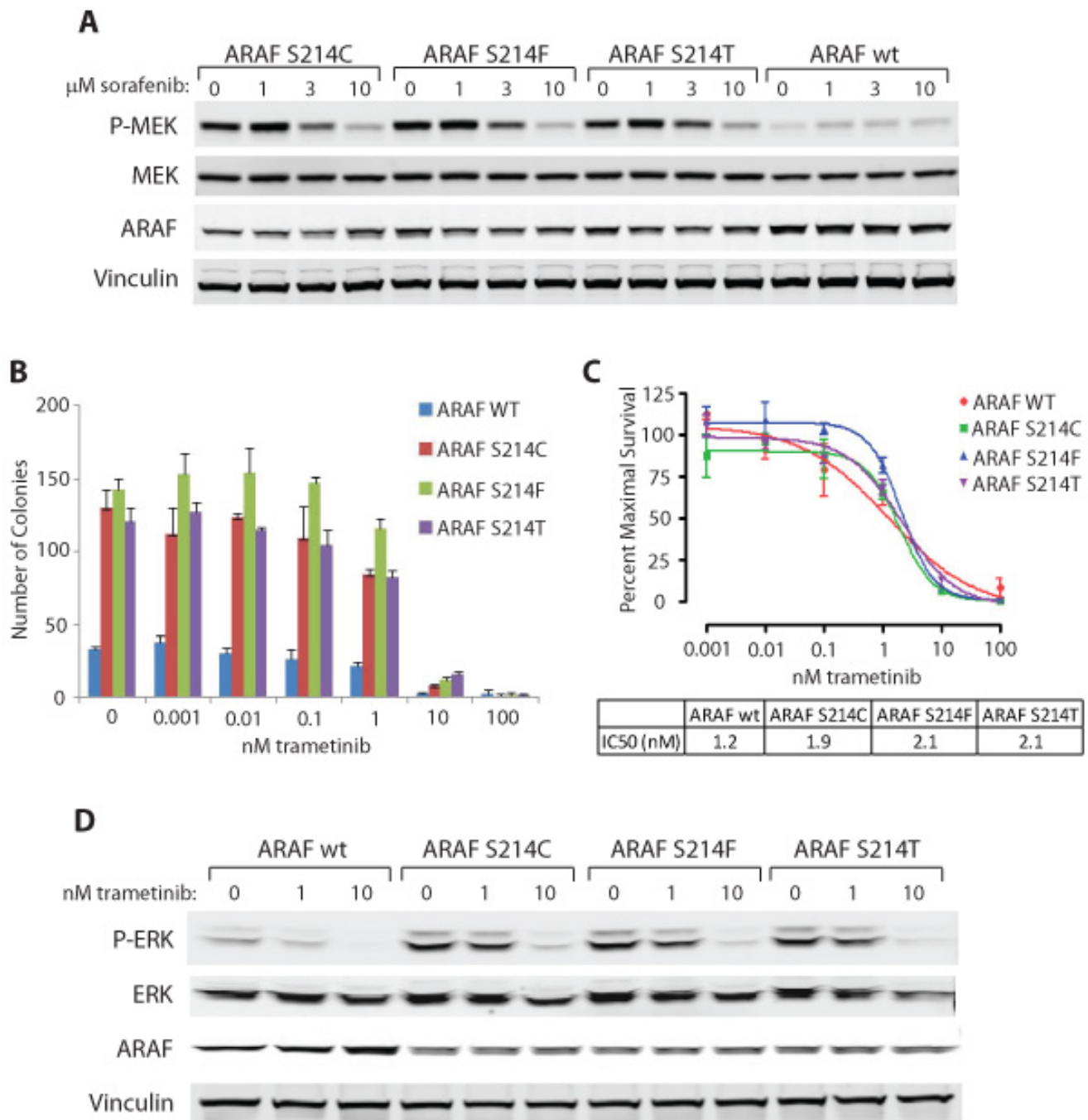
RAF1 mutations at S257 and S259 are activating and oncogenic. (A) Soft agar colony formation by NIH-3T3 cells ectopically expressing variants of *RAF1*. (B) Immunoblot of RAF1 protein expression in cells used for soft agar assay shown in panel (A). (C) Soft agar colony formation by AALE cells ectopically expressing variants of RAF1. (D) Immunoblot of RAF1 protein expression and Mek phosphorylation in cells used for soft agar assay shown in panel (C). PBP, empty vector; WT, wild-type; K375M, kinase-inactive RAF1.
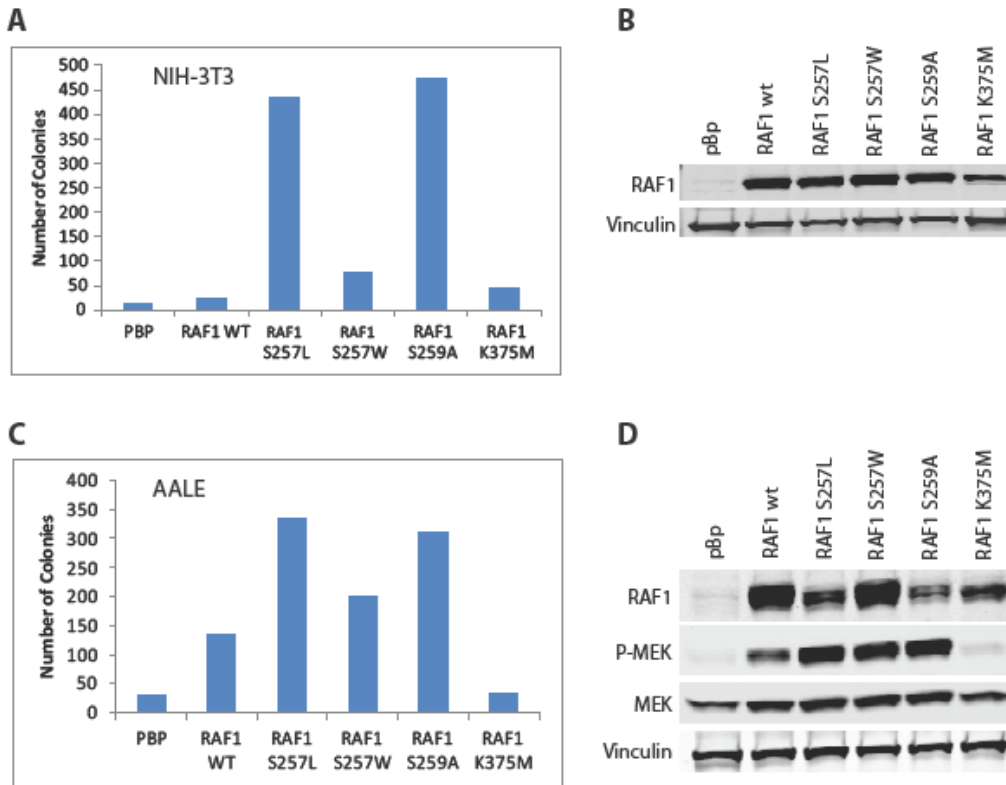
RAF1 mutations are sensitive to sorafenib and trametinib. (A) Dose response curve of RAF1 AALE cells treated with the indicated concentrations of sorafenib. (B) Dose response curve of RAF1 AALE cells treated with the indicated concentrations of trametinib. Data and error bars in panels (A),(B) represent mean ± SEM, respectively, obtained from triplicate experiments. (C) MEK phosphorylation is decreased in response to sorafenib treatment. Immunoblots from AALE cells ectopically expressing *RAF1* mutants treated with the indicated concentrations of sorafenib for 4 hours. (D) Erk phosphorylation is decreased in response to trametinib treatment. Immunoblots from AALE cells ectopically expressing *RAF1* mutants treated with the indicated concentrations of trametinib for 2 hours.

	RAF1 wt	RAF1 S257L	RAF1 S257W	RAF1 S259A
IC50 (µM)	0.6	0.9	0.9	1.1
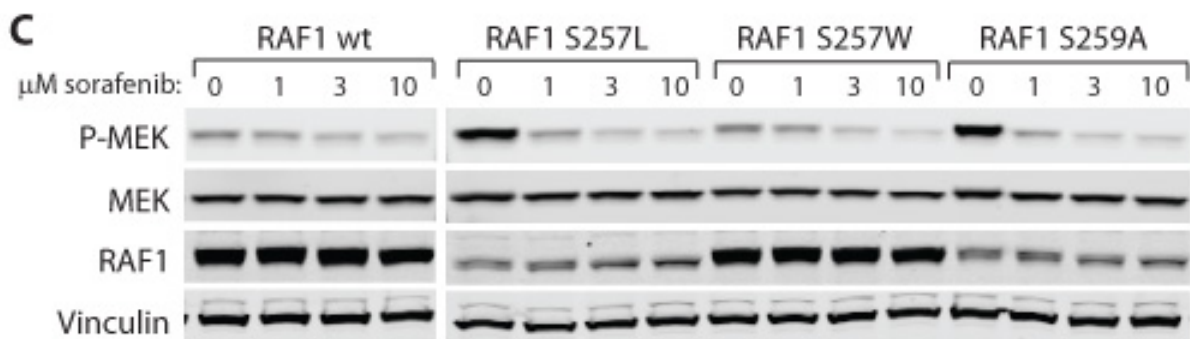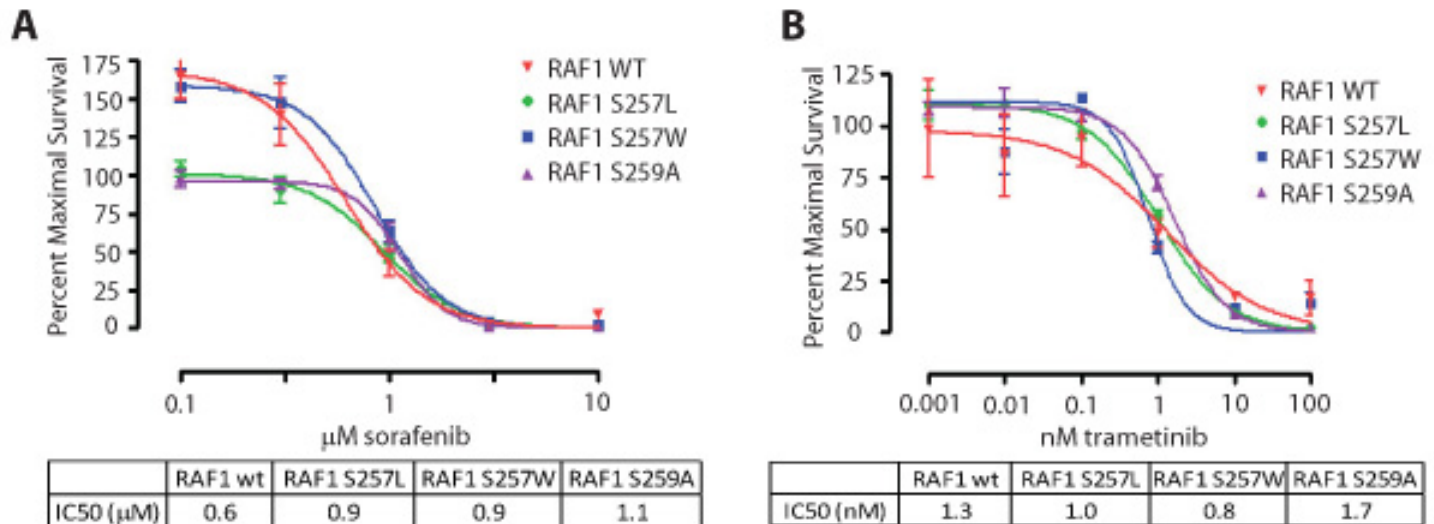
	RAF1 wt	RAF1 S257L	RAF1 S257W	RAF1 S259A
IC50 (nM)	1.3	1.0	0.8	1.7

Mutation of ARAF S214 decreases 14-3-3 binding. Lysates from ARAF AALE cells were incubated with 1 μg GST-14-3-3ζ, precipitated with glutathione agarose, and immunoblotted for associated ARAF protein. ARAF S214C exhibits decreased co-precipitation with 14-3-3ζ compared to wild-typ ARAF. pBp, empty pBabe-puro vector; wt, wild-type.
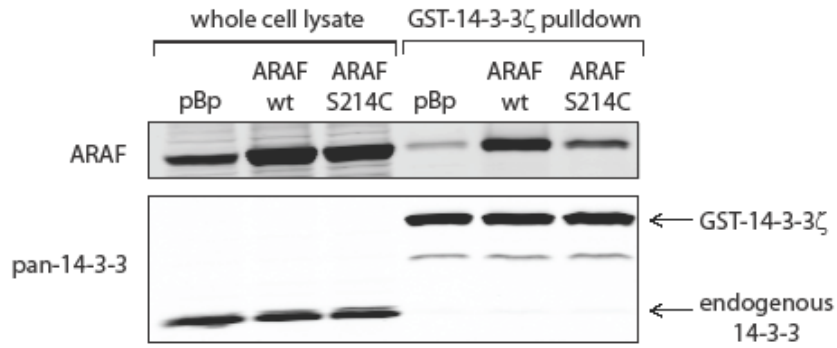
Supplemental Tables

<u>Supplemental Table 1:</u> Somatic and germline coding substitution and small insertion-deletion variants identified from WGS of tumor and peripheral blood sample profiled in this study. This table is provided as a file attachment (Supp Table 1.xlsx)

<u>Supplemental Table 2:</u> Somatic rearrangements identified from WGS of tumor and peripheral blood sample profiled in this study. Each row of the table represents a pair of signed loci that are predicted to be fused through paired-end and split-read analysis via dRanger and BreakPointer tools(2-4).   By convention, fusions refer to the joining of the sequences in the 3' direction on the specified strand (i.e. '+' refers to the sequence to the right, or in the direction of increasing position, on the reference genome, and '-' refers to the sequence to the left, or in the direction of decreasing position on the reference).   Coordinates are given in hg19 coordinates. This table is provided as a file attachment (Supp Table 2.xlsx).

Supplemental Table 3: Copy number alterations identified from WGS of tumor and peripheral blood sample profiled in this study. Each row specifies an interval of the reference genome and is associated with a continuous abundance (tumor / normal read depth ratio) and inferred integer copy state. This table is provided as a file attachment (Supp Table 3.xlsx)

Supplemental Table 4: The somatic variant, tumor gene expression, and coding germline variant data at 29 known sorafenib target genes is shown. This gene set was obtained from the results of a published *in vitro* kinase profiling study(27) by including all kinase genes demonstrating 20% or greater relative inhibition of catalytic activity from baseline in the presence of 0.5 µM sorafenib. Expression results are provided as fragments per kilobase per million mapped reads (FPKM)(6). Germline coding variants are annotated with their protein and genomic variant name, as well as dbSNP ID (http://www.ncbi.nlm.nih.gov/projects/SNP/), 1000 genomes allele fraction(28) (AF), PolyPhen2 score and classification (PPH2)(29), when available. All coding germline variants in these genes were either common (AF > 0.05) or neutral by PolyPhen2. There were no rearrangements involving a sorafenib target gene; as a result this column is not included in the table.

Gene	Chr	Start	End	Somatic CN	Tumor Gene Expression (FPKM)	Somatic Mutations	Germline variants
ARAF	X	47420515	47431319	5	24.04	p.S214C	
AURKB	17	8108049	8113883	4	2.91		p.M298T (g.17:8108331A>G, rs1059476, AF: 0.75)
BRAF	7	140433814	140624564	3	1.77		
CSF1R	5	149432854	149492935	3	0.00		p.H362R (g.5:149450132T>C, rs10079250, AF: 0.16, PPH2: 0.008, neutral)
DDR2	1	162602227	162750237	4	0.00		p.V555G (g.1:162741973T>G, rs77232496, PPH2: 0.263, neutral)
EPHA6	3	96533424	97467786	3	0.10		
FGFR2	10	123237844	123357972	3	1.11		
FLT1	13	28874482	29069265	3	6.10		
FLT3	13	28577411	28674729	3	0.09		p.T227M (g.13:28624294G>A, rs1933437 AF:0.57, PPH2: 0.993, deleterious)
FLT4	5	180028506	180076624	3	3.33		p.H890Q (g.5:180046344G>C, rs448012, AF: 0.47, PPH2: 0.714, deleterious)
HIPK4	19	40885178	40896094	3	0.01		
KDR	4	55944426	55991762	5	4.35		p.Q472H (g.4:55972974T>A, rs1870377, AF:0.24, PPH2: 0, neutral) ; p.V297I (g.4:55979558C>T, rs2305948 AF:0.13, PPH2: 0.97, deleterious)
KIT	4	55524094	55606879	5	53.42		
LIMK1	7	73498155	73536854	3	2.69		
MAP4K5	14	50885246	50999376	3	0.00		
MAPK11	22	50702142	50708779	2	0.00		
MAPK14	6	35995453	36079012	6	6.49		
MKNK1	1	47023090	47069966	4	10.85		
MKNK2	19	2037469	2051243	2	6.94		
NTRK1	1	156785541	156851642	4	0.00		
NTRK3	15	88419987	88799661	3	0.00		
PDGFRA	4	55095263	55164411	5	2.41		
PDGFRB	5	149493402	149535422	3	11.44		
RAF1	3	12625101	12705700	3	14.28		
RET	10	43572516	43625795	3	0.00		
STK10	5	171469073	171615346	4	0.36		
TAOK2	16	29985221	30003581	4	7.76		p.R1211H (g.16:29999225G>A, rs11864149, AF:0.08, PPH2: 0.276, neutral)
TAOK3	12	118587606	118810750	3	1.85		p.S47N (g.12:118682751C>T, rs428073, AF:0.29, PPH2: 0, neutral)
ZAK	2	173940564	174132736	4	0.96		p.S531L (g.2:174128513C>T, rs3769148, AF:0.28)

<u>Supplemental Table 5</u>: Somatic *ARAF* and *RAF1* mutations in lung adenocarcinoma and 11 other tumor types profiled by TCGA (http://cancergenome.nih.gov/) and Imielinski et al(21).   The final column of the table shows co-occurring somatic mutations in selected activating oncogenes for each patient harboring the given *ARAF* / *RAF1* somatic event.   This table is provided as a file attachment (Supp Table 5.xlsx)

Supplemental Table 6: Estimates and confidence intervals for concentrations of sorafenib and trametenib causing 50% inhibition of maximal colony formation (IC50) for in AALE cells over-expressing wild type or mutant ARAF.

	ARAF wt	ARAF S214C	ARAF S214F	ARAF S214T
sorafenib IC50 (μM)	1.1	1.1	1.1	1.3
95% confidence interval (μM)	0.8-1.7	0.7-1.7	0.9-1.3	1.0-1.6
trametinib IC50 (nM)	1.24	1.90	2.08	2.12
95% confidence interval (nM)	0.19-7.96	0.79-4.59	1.16-3.72	1.12-3.87

References

1. Meyerson, M., Gabriel, S., and Getz, G. 2010. Advances in understanding cancer genomes through second-generation sequencing. *Nat Rev Genet* 11:685-696.
2. Cibulskis, K., Lawrence, M.S., Carter, S.L., Sivachenko, A., Jaffe, D., Sougnez, C., Gabriel, S., Meyerson, M., Lander, E.S., and Getz, G. 2013. Sensitive detection of somatic point mutations in impure and heterogeneous cancer samples. *Nat Biotechnol* 31:213-219.
3. Chiang, D.Y., Getz, G., Jaffe, D.B., O'Kelly, M.J., Zhao, X., Carter, S.L., Russ, C., Nusbaum, C., Meyerson, M., and Lander, E.S. 2009. High-resolution mapping of copy-number alterations with massively parallel sequencing. *Nat Methods* 6:99-103.
4. Carter, S.L., Cibulskis, K., Helman, E., McKenna, A., Shen, H., Zack, T., Laird, P.W., Onofrio, R.C., Winckler, W., Weir, B.A., et al. 2012. Absolute quantification of somatic DNA alterations in human cancer. *Nat Biotechnol* 30:413-421.
5. DePristo, M.A., Banks, E., Poplin, R., Garimella, K.V., Maguire, J.R., Hartl, C., Philippakis, A.A., del Angel, G., Rivas, M.A., Hanna, M., et al. 2011. A framework for variation discovery and genotyping using next-generation DNA sequencing data. *Nat Genet* 43:491-498.
6. Trapnell, C., Roberts, A., Goff, L., Pertea, G., Kim, D., Kelley, D.R., Pimentel, H., Salzberg, S.L., Rinn, J.L., and Pachter, L. 2012. Differential gene and transcript expression analysis of RNA-seq experiments with TopHat and Cufflinks. *Nat Protoc* 7:562-578.
7. Li, H., Handsaker, B., Wysoker, A., Fennell, T., Ruan, J., Homer, N., Marth, G., Abecasis, G., and Durbin, R. 2009. The Sequence Alignment/Map format and SAMtools. *Bioinformatics* 25:2078-2079.
8. Krzywinski, M., Schein, J., Birol, I., Connors, J., Gascoyne, R., Horsman, D., Jones, S.J., and Marra, M.A. 2009. Circos: an information aesthetic for comparative genomics. *Genome Res* 19:1639-1645.
9. Suzuki, Y., Kagawa, N., Fujino, T., Sumiya, T., Andoh, T., Ishikawa, K., Kimura, R., Kemmochi, K., Ohta, T., and Tanaka, S. 2005. A novel high-throughput (HTP) cloning strategy for site-directed designed chimeragenesis and mutation using the Gateway cloning system. *Nucleic Acids Res* 33:e109.
10. Kamentsky, L., Jones, T.R., Fraser, A., Bray, M.A., Logan, D.J., Madden, K.L., Ljosa, V., Rueden, C., Eliceiri, K.W., and Carpenter, A.E. 2011. Improved structure, function and compatibility for CellProfiler: modular high-throughput image analysis software. *Bioinformatics* 27:1179-1180.
11. Greulich, H., Kaplan, B., Mertins, P., Chen, T.H., Tanaka, K.E., Yun, C.H., Zhang, X., Lee, S.H., Cho, J., Ambrogio, L., et al. 2012. Functional analysis of receptor tyrosine kinase mutations in lung cancer identifies oncogenic extracellular domain mutations of ERBB2. *Proc Natl Acad Sci U S A* 109:14476-14481.
12. Weir, B.A., Woo, M.S., Getz, G., Perner, S., Ding, L., Beroukhim, R., Lin, W.M., Province, M.A., Kraja, A., Johnson, L.A., et al. 2007. Characterizing the cancer genome in lung adenocarcinoma. *Nature* 450:893-898.
13. Seo, J.-S., Ju, Y.S., Lee, W.-C., Shin, J.-Y., Lee, J.K., Bleazard, T., Lee, J., Jung, Y.J., Kim, J.-O., Shin, J.-Y., et al. 2012. The transcriptional landscape and mutational profile of lung adenocarcinoma. *Genome Res*.
14. Liu, J., Lee, W., Jiang, Z., Chen, Z., Jhunjhunwala, S., Haverty, P.M., Gnad, F., Guan, Y., Gilbert, H.N., Stinson, J., et al. 2012. Genome and transcriptome sequencing of lung cancers reveal diverse mutational and splicing events. *Genome Research* 22:2315-2327.
15. Lee, W., Jiang, Z., Liu, J., Haverty, P.M., Guan, Y., Stinson, J., Yue, P., Zhang, Y., Pant, K.P., Bhatt, D., et al. 2010. The mutation spectrum revealed by paired genome sequences from a lung cancer patient. *Nature* 465:473-477.

16. Kan, Z., Jaiswal, B.S., Stinson, J., Janakiraman, V., Bhatt, D., Stern, H.M., Yue, P., Haverty, P.M., Bourgon, R., Zheng, J., et al. 2010. Diverse somatic mutation patterns and pathway alterations in human cancers. *Nature* 466:869-873.

17. Kohno, T., Ichikawa, H., Totoki, Y., Yasuda, K., Hiramoto, M., Nammo, T., Sakamoto, H., Tsuta, K., Furuta, K., Shimada, Y., et al. 2012. KIF5B-RET fusions in lung adenocarcinoma. *Nat Med*.

18. Govindan, R., Ding, L., Griffith, M., Subramanian, J., Dees, N.D., Kanchi, K.L., Maher, C.A., Fulton, R., Fulton, L., Wallis, J., et al. 2012. Genomic landscape of non-small cell lung cancer in smokers and never-smokers. *Cell* 150:1121-1134.

19. Ding, L., Getz, G., Wheeler, D.A., Mardis, E.R., Mclellan, M.D., Cibulskis, K., Sougnez, C., Greulich, H., Muzny, D.M., Morgan, M.B., et al. 2008. Somatic mutations affect key pathways in lung adenocarcinoma. *Nature* 455:1069-1075.

20. Beroukhim, R., Mermel, C.H., Porter, D., Wei, G., Raychaudhuri, S., Donovan, J., Barretina, J., Boehm, J.S., Dobson, J., Urashima, M., et al. 2010. The landscape of somatic copy-number alteration across human cancers. *Nature* 463:899-905.

21. Imielinski, M., Berger, A.H., Hammerman, P.S., Hernandez, B., Pugh, T.J., Hodis, E., Cho, J., Suh, J., Capelletti, M., Sivachenko, A., et al. 2012. Mapping the hallmarks of lung adenocarcinoma with massively parallel sequencing. *Cell* 150:1107-1120.

22. Lawrence, M.S., Stojanov, P., Polak, P., Kryukov, G.V., Cibulskis, K., Sivachenko, A., Carter, S.L., Stewart, C., Mermel, C.H., Roberts, S.A., et al. 2013. Mutational heterogeneity in cancer and the search for new cancer-associated genes. *Nature* 499:214-218.

23. Alexandrov, L.B., Nik-Zainal, S., Wedge, D.C., Aparicio, S.A., Behjati, S., Biankin, A.V., Bignell, G.R., Bolli, N., Borg, A., Borresen-Dale, A.L., et al. 2013. Signatures of mutational processes in human cancer. *Nature* 500:415-421.

24. Davies, H., Bignell, G.R., Cox, C., Stephens, P., Edkins, S., Clegg, S., Teague, J., Woffendin, H., Garnett, M.J., Bottomley, W., et al. 2002. Mutations of the BRAF gene in human cancer. *Nature* 417:949-954.

25. Forbes, S.A., Tang, G., Bindal, N., Bamford, S., Dawson, E., Cole, C., Kok, C.Y., Jia, M., Ewing, R., Menzies, A., et al. 2010. COSMIC (the Catalogue of Somatic Mutations in Cancer): a resource to investigate acquired mutations in human cancer. *Nucleic Acids Res* 38:D652-657.

26. Michaud, N.R., Fabian, J.R., Mathes, K.D., and Morrison, D.K. 1995. 14-3-3 is not essential for Raf-1 function: identification of Raf-1 proteins that are biologically activated in a 14-3-3- and Ras-independent manner. *Mol Cell Biol* 15:3390-3397.

27. Anastassiadis, T., Deacon, S.W., Devarajan, K., Ma, H., and Peterson, J.R. 2011. Comprehensive assay of kinase catalytic activity reveals features of kinase inhibitor selectivity. *Nat Biotechnol* 29:1039-1045.

28. Abecasis, G.R., Altshuler, D., Auton, A., Brooks, L.D., Durbin, R.M., Gibbs, R.A., Hurles, M.E., and McVean, G.A. 2010. A map of human genome variation from population-scale sequencing. *Nature* 467:1061-1073.

29. Adzhubei, I.A., Schmidt, S., Peshkin, L., Ramensky, V.E., Gerasimova, A., Bork, P., Kondrashov, A.S., and Sunyaev, S.R. 2010. A method and server for predicting damaging missense mutations. *Nat Methods* 7:248-249.